Published in final edited form as:
Bone. 2009 March ; 44(3): 502–512. doi:10.1016/j.bone.2008.11.012.

Periostin-Like-Factor and Periostin in an Animal Model of Work-Related Musculoskeletal Disorder

Shobha Rani[1], **Mary F. Barbe**[1,3,4], **Ann E. Barr**[2], and **Judith Litvin**[1,4]

[1]Department of Anatomy and Cell Biology, Temple University School of Medicine, Philadelphia, PA, 19140

[2]Department of Physical Therapy, Thomas Jefferson University, Philadelphia, PA, 19107

[3]Department of Physical Therapy, Temple University, Philadelphia, PA, 19140

Abstract

Work-related musculoskeletal disorders (WMSDs), also known as overuse injuries, account for a substantial proportion of work injuries and workers' compensation claims in the United States. However, the pathophysiological mechanisms underlying WMSDs are not well understood, especially the early events in their development. In this study we used an animal model of upper extremity WMSD, in which rats perform a voluntary repetitive reaching and pulling task for a food reward. This innovative model provides us an opportunity to investigate the role of molecules which may be used either as markers of early diagnosis of these disorders, and/or could be targeted for therapeutic purposes in the future. Periostin-Like-Factor (PLF), and Periostin were examined in this study. Both belong to a family of vitamin K-dependent gamma carboxylated proteins characterized by the presence of conserved Fasciclin domains and not detected in adult tissues except under conditions of chronic overload, injury, stress or pathology. The spatial and temporal pattern of PLF and Periostin localization was examined by immunohistochemistry and western blot analysis in the radius and ulna of animals performing a high repetition, high force task for up to 12 weeks and in controls. We found that PLF was present primarily in the cellular periosteum, articular cartilage, osteoblasts, osteocytes and osteoclasts at weeks 3 and 6 in all distal bone sites examined. This increase coincided with a transient increase in serum osteocalcin in week 6, indicative of adaptive bone formation at this time point. PLF immunoexpression decreased in the distal periosteum and metaphysis by week 12, coincided temporally with an increase in serum Trap5b, thinning of the growth plate and reduced cortical thickness. In contrast to PLF, once Periostin was induced by task performance, it continued to be present at a uniformly high level between 3 and 12 weeks in the trabeculae, fibrous and cellular periosteum, osteoblasts and osteocytes. In general, the data suggest that PLF is located in tissues during the early adaptive stage of remodeling but not during the pathological phase and therefore might be a marker of early adaptive remodeling.

Correspondence to: Judith Litvin, Ph.D. Temple University School of Medicine, Department of Anatomy and Cell Biology, 3400 N. Broad St. Philadelphia, PA 19140, 215-707-2070, Judith.litvin@temple.edu.
[4]Equally Contributing Authors

Keywords

Work-related musculoskeletal disorder; Periostin-Like-Factor; Periostin; Bone; Epiphyseal plate; Periosteum

Introduction

Periostin and periostin-like-factor (PLF) are part of a family of vitamin K-dependent gamma carboxylated proteins that contain 150 amino acid long repeat domains (RDs) and are evolutionarily conserved [1–3]. Members of this family include Fasciclin I identified in insects [1], Algal-CAM in the algae Volvox [4], MPB-70 in bacteria *Mycobacterium bovis* [5], and Stabilins I & II, βigH3, Periostin and Periostin-like-factor (PLF) in higher order vertebrates [6–9]. Differences between isoforms in this family of proteins, determined using nucleic acid and predicted amino acid sequence analyses, are located in the COOH-terminus [2, 8, 9]. Periostin and PLF, the two most commonly studied members of this family are induced in various pathologies, making them potential targets and/or markers in disease. These two proteins are single gene products and differ in their COOH terminal region [2, 8, 9]. Neither PLF nor Periostin are expressed in most adult tissues under normal conditions, but is expressed under conditions of mechanical overload or injury and repair of the musculoskeletal system, and in disease of the cardiovascular system [9–21]. Both isoforms are induced in adult tissues and cells under adverse conditions such as hypoxia, UV exposure, serum starvation, abnormal cell growth and pressure or volume and mechanical overload. Periostin is also induced under various pathological conditions like cardiovascular disease, oncogenesis and fibrogenesis. For example, Periostin is expressed in adult after balloon injury in carotid arteries, at sites of pathologic myocardial remodeling, and when the heart is subjected to pressure overload [10, 12, 20–24]. With respect to oncogenesis, Periostin is increased in oral squamous cell carcinoma, pancreatic ductal adenocarcinoma, head and neck cancer, stage IV thymoma, pancreatic cancer, liver cancer, and in melanoma cells [25–30]. Several human brain tumors, breast cancers, non-small cell lung carcinomas, ovary and colon cancers also show upregulation of Periostin [31–38] and its tumor suppressor activity lies in the COOH-terminus [39]. In pancreatic tumors, Periostin promotes fibrogenic activity and supports tumor cell growth under conditions of serum deprivation and hypoxia [40]. With respect to fibrotic conditions, Periostin plays a role in bone marrow fibrosis and is a component of sub-epithelial fibrosis in bronchial asthma in which it regulates collagen fibrillogenesis and determines the biomechanical properties of connective tissues by regulating collagen fiber diameter and cross-linking [41–43]. Thus, Periostin is induced and plays varied roles in adult tissues under pathological conditions or mechanical stress.

The isoform PLF is expressed in adult tissues only after exposure to trauma or pathology. For example, PLF is induced in failing human hearts, and in rat hearts under volume overload [20]. Similarly, in adult bone PLF is up regulated under conditions of fracture healing [44]. In general, it appears that PLF is up regulated in adult tissues exposed to damage, tissue trauma, overload, and/or stress.

With this in mind, we sought to examine the temporal and spatial presence of these two proteins in a rat model of work-related musculoskeletal disorders (WMSDs), which are also known as overuse injuries or repetitive strain injuries, that account for a substantial proportion of work injuries and workers' compensation claims in the United States [45]. The US Department of Labor defines WMSDs as injuries or disorders of muscles, nerves, tendons, ligaments, bone, joints, cartilage, and spinal discs associated with exposure to risk factors in the workplace. Factors associated with the development of these injuries include

physical, biomechanical and/or genetic factors [46, 47]. Examples of overuse injuries include sprains, strains, tears, stress fractures and carpal tunnel syndrome [45]. The key to controlling the impact of such disorders is prevention or early intervention. However, to plan effective treatments or interventions the pathophysiological mechanisms underlying WMSDs must be understood, especially the early events in their development. Animal models provide an ideal system to study the initiation and progress of these events at all stages. One such animal model of upper extremity WMSD in which rats perform a voluntary repetitive reaching and grasping task for a food reward was developed by Barr and Barbe [48]. Using this model, it has already been shown that performance of repetitive motion tasks leads to injury of musculotendinous tissues and peripheral nerves, carpal tunnel syndrome with extraneural fibrosis and decreased nerve conduction, and motor declines [49–55]. This innovative model provides us with an opportunity to investigate the role of molecules which may be used either as markers of early diagnosis of these disorders, and/or could be targeted for therapeutic purposes in the future.

Since both PLF and Periost in are induced under conditions of overload, we hypothesize that they may be used as markers of musculoskeletal overload and/or pathology. We further hypothesize that both PLF and Periostin levels will increase after the performance of high demand repetitive tasks. In this study, we explore the presence of PLF and Periostin in forelimb bones after performance of a high repetition, high force reaching and pulling task and show that each has a unique spatial and temporal localization pattern in the reach limb in this animal model of WMSD. We also show that PLF increases during the early adaptive stage of bone remodeling.

Materials and Methods

Subjects

Adult female Sprague–Dawley rats (3.5 months of age at onset of experiments) were obtained from ACE, PA. The animals were housed in the Central Animal Facility on the Health Sciences Campus at Temple University. Animal care and use was monitored by the University Animal Care and Use Committee to assure compliance with the provisions of Federal Regulations and the NIH “Guide for the Care and Use of Laboratory Animals”. Experimental and age-and-weight yoked trained control rats were weighed two to three times per week, provided rat chow daily to supplement the purified formula pellets (Bioserve, Frenchtown, NJ) used for food reward, to maintain their weight, and given free access to water throughout the experiment.

Behavioral apparatus and repetitive motion task requirements

The force apparatus was custom-designed (by Dr. Ann Barr and Custom Medical Research Equipment, Glendora, NJ) and integrated into an existing commercially available operant training system (Med Associates, Georgia, VT). Detailed specifications of the testing chamber and force apparatus are as described previously [49]. Experimental rats performed a high repetition high force task regimen of 12 reaches/min at 60 ± 5% maximum pulling force (MPF). Using auditory and light cues, rats were cued to reach every 7.5 sec, which is a target rate of 8 reaches/min; however, most of the animals tended to overreach and averaged 12 reaches/min. In terms of force criteria, rats were trained to pull a force handle between minimum (55% of maximum pulling force (MPF), as determined in control rats, and maximum (65% MPF) force criterion for at least 50 ms. If these force and time criteria were met, a reward light was turned on and a food pellet was dispensed into a trough, which the rat could only reach by releasing the handle. MPF was determined on the last day of the initial training period during a 5 min session in which the force criterion for a food reward was gradually increased. Animals were observed carefully for their maximum force

generating ability during this 5 minute session, and MPF was selected as the highest force resulting in a successful reach (i.e., food pellet reward) that could be repeated 3 times.

Training and repetitive motion task performance

Fifty rats were randomized into one of 3 groups: A high repetition high force group (HRHF; n=32), a normal control group (NC; n=9), or a trained control group (TC; n=9). A power analysis was performed using prior published data from our laboratory, which indicated that n=4 was sufficient for 80% power. The HRHF and trained control rats learned to reach for the food during an initial 4 to 6 week training period. Rats were trained to perform a repetitive handle-pulling task with food reward using standard operant conditioning procedures during the training period in which access to food was restricted in order to motivate them to learn the task. Some animals may have undergone a short period (no more than 7 days) of weight reduction to no less than 80% of the weights of the age-matched normal control group with free access to food. Once the animals learned the task, they rapidly gained weight and were maintained at ± 5% of age-matched control rats' weights (rats with free access to food). Rats were weighed at least twice weekly and rat chow adjusted accordingly.

During an initial training period, the animals were first encouraged to reach through open bars for food pellets placed on an elevated platform for 5 min/day. When they began to reach freely for the food, they were transferred to the test chamber until they could reach into the tube dispenser with no specified reach rate for 10 to 20 min/day. Both TC and HRHF task rats were trained to achieve at least 8 reaches/min for 10 to 20 min/day; however, to repeat from above, most tended to overreach and averaged 12 reaches/min. The TC rats were age and weight-matched to HRHF task rats, but did not perform beyond this initial training period. The TC rats were euthanized at the 12 week endpoint at time points matched to the 12 week HRHF rats.

Once the animals were able to perform the task consistently, typically after a total training period of 4 to 6 weeks, the HRHF experimental animals began the task regimen at the rate of 12 reaches/min at 60 ± 5% maximum pulling force (MPF), for 2 hr/day, 3 days/week (Monday, Wednesday, Friday) for 3, 6, 8 or 12 weeks. The daily task was divided into four, 0.5-hr training sessions separated by 1.5 hr. Animals were allowed to use their preferred limb to reach. The side used to reach was recorded for each session.

Collection of serum for biomarker analyses

Serum was collected from 34 rats: normal controls (NC, n =8), trained controls rats (TC; n=6), and rats that performed the HRHF task for 6 (n=8) or 12 weeks (n=6). Following euthanasia (Nembutal, 120 mg/kg body weight), 18–36 hours after completion of the final task session, blood was collected by cardiac puncture using a 23-gauge needle. The blood was centrifuged immediately at 1000 g for 20 min at 4°C. Serum was collected, separated into 200 μl aliquots, flash-frozen, and stored at −80°C until analyzed. Levels of osteocalcin and tartrate-resistant acid phosphatase 5b (Trap5b) were analyzed in serum using commercially available ELISA kits (NB Bioscience and Immunodiagnostics) according to the manufacturer's protocols.

Collection of tissues for immunohistochemical and morphological analyses

Animals were euthanized (Nembutal, 120 mg/kg body weight) and perfused transcardially with 4% paraformaldehyde in 0.1 M phosphate buffer (pH 7.4). These methods are consistent with the recommendations of the Panel on Euthanasia of the American Veterinary Medical Association. Rats performing the HRHF task were euthanized at 3 (n = 4), 6 (n = 4), 8 (n = 4) or 12 (n = 4) weeks, as were normal control (NC; n = 4) and trained control

(TC; $n = 4$) rats. Tissues from the preferred reach limbs were collected and postfixed "en bloc" by immersion overnight. Forearm radius and ulna bones were collected; decalcified, paraffin embedded, and sectioned as described previously [44, 51].

Immunohistochemistry and quantification

Longitudinal sections through the center of the radius and ulna were treated with 3% H_2O_2 in methanol for 30 min, washed, and then blocked with 4% goat serum in phosphate buffered saline and 0.1% Triton-X100 (PBST) for 30 min at room temperature. Sections were then incubated overnight at 4 °C with primary antibody diluted in 5% goat serum/PBS. Primary anti-PLF and Periostin were used at a 1:1000 and 1:750 dilution, respectively. Specificity of the primary antibodies has been previously described [56]. After washing, sections were incubated with secondary antibody, diluted 1:500 for 30 min at room temperature. The sections were then washed and treated for 30 min with signal amplification kit, (ABC kit, Vector laboratories), signal was visualized using diaminobenzidine (DAB). DAB-treated sections were counterstained with hematoxylin and examined using bright field microscopy. Negative control staining was performed by omitting the primary antibody.

Positive stain for PLF or Periostin was quantified using a microscope interfaced with an image analysis system (Bioquant Osteo II) using a videocount thresholding method described previously [53]. Briefly, immunohistochemical (DAB) stained slides were analyzed using the videocount area, irregular region of interest tool, and field mode options of Bioquant Osteo II using similar videocount thresholding methods as described previously [53]. The video count area is the number of pixels in a field that meet a user defined criterion multiplied by the area of a pixel at the selected magnification. The mean area fraction of thresholded immunoreactive product in a selected region of interest was determined by dividing the videocount area of pixels above background thresholds by the videocount area of all pixels in the entire chosen field. Two field counts were made of each tissue of interest in 3 sections per rat using a 20X objective for a total of 6 field counts per tissue/rat. Four rats were analyzed using this approach per group giving n=4/group for statistical analysis. Group means and standard error of the mean were plotted against weeks of task performance and are expressed as percent area fraction of immunostaining. Univariate ANOVAs (Prism Software) were used to determine whether weeks of task performance had an effect on PLF levels in bones. A p value of < 0.05 was considered significant for all analyses.

Morphological analysis

Longitudinal sections through the center of the radius and ulna were analyzed, after collection and preparation as described above, using the auto width measurement tool combined with irregular region of interest tool of Bioquant Osteo II to measure mean cortical thickness and mean growth plate height of the distal radius and ulna. Three fields were measured using a 20x objective in at least two, typically three, nonadjacent sections from each animal. An average of 18 measurements were made per field at 20 μm intervals using the Bioquant auto width measurement tool, and averaged. The proximal growth plate was not analyzed since it had already undergone closure, and was no longer present in these young adult rats. Only bones from the reach limb were analyzed. Hematoxylin and eosin stained sections were used for these analyses.

Western blot analysis

Additional cohorts of rats from those used for immunohistochemistry were euthanized with an overdose of sodium pentobarbital (Nembutal; 120 mg/kg body weight). Forearm bones (radius and ulna) were collected from rats that had performed the HRHF task for 3, (n=3), 6 (n =3) or 8 (n =3), or 12 weeks (n =3), and normal controls (n=3) and trained control rats

(n=3). The forearm bones were further divided into distal and proximal portions (the distal part consisting of the radius/ulna metaphyses and epiphyses and first row of carpal bones; the proximal part consisting of radius/ulna diaphyses). Bones pieces were homogenized in RIPA buffer [25 mM Tris•HCl pH 7.6, 150 mM NaCl, 1% NP-40, 1% sodium deoxycholate, 0.1% SDS, protease inhibitor cocktail (Sigma)], incubated overnight at 4°C, supernatant collected and stored at −80°C. For western blot analysis 25 μg of protein sample was mixed with 5X Laemmli sample buffer (10% SDS, 50% Glycerol, 25% β mercaptoethanol, 300mM Tris HCl pH 6.8, and 0.04% Bromophenol blue), boiled for 5 minutes, and resolved by 10% SDS-PAGE. Protein samples were transferred to a nitrocellulose membrane at 90Volts for 1 hr at 4°C, the membrane was blocked in 5% non-fat dry milk in phosphate-buffered saline (PBS) with 0.1% Tween-20 (PBST) for 1 hour and incubated in 0.3μg/ml Periostin-specific primary antibody overnight at 4°C [56]. The membrane was washed with PBST, incubated with 0.2μg/ml of HRP-conjugated goat anti-rabbit IgG secondary antibody (Pierce, Rockford, IL) for 1 hour at room temperature, and the chemiluminescent signal was detected using the ECL kit (Pierce, Rockford, IL). Blots were stripped, washed and reprobed with 0.2 μg/ml GAPDH-specific primary antibodies overnight at 4°C. The membrane was washed with PBST and incubated with 0.2μg/ml of HRP-conjugated goat anti-mouse IgG secondary antibody (Pierce, Rockford, IL) for 1 hour at room temperature, and the chemiluminescent signal was detected using the ECL kit (Pierce, Rockford, IL).

Results

Task Performance leads to up regulation of PLF but not Periostin in the epiphyseal plate

PLF and Periostin levels are up regulated under conditions of tissue overload and stress [8, 18–20, 59]. Therefore, we hypothesized that PLF and Periostin may be induced in our animal model of upper-extremity WMSD and by immunohistochemical analyses we determined the temporal and spatial location of these proteins.

PLF was not detected in the epiphyseal plates of the radius and ulna from normal control animals (Fig 1A). However, the protein was present at low levels in these bones of trained control animals in both the epiphyseal plate and bony trabeculae in the bone marrow cavity (Fig 1B). When animals performed the HRHF task, PLF was detected at significantly high levels at weeks 3, 6 and 12 in the radius and ulna epiphyseal plates but was not detected at 8 weeks (Figs 1C, D, F versus 1E). At 3 weeks of task performance, it was secreted by proliferating chondrocytes (Fig 1C), at 6 weeks by prehypertrophy and hypertrophy chondrocytes (Fig 1D) and at 12 weeks by hypertrophied chondrocytes (Fig 1F). PLF was also detected in distal bony trabeculae in the bone marrow cavity of these same bones at 3, 6 and 12 weeks of task performance (Fig 1C, D, F) and at lower levels at week 8 (Fig 1E). Thus, PLF localization in the distal epiphyseal plate and trabecular bone of radii and ulna had a distinct temporal and spatial pattern in response to task performance. Bioquant analysis confirmed that PLF was induced in the epiphyseal plate at low levels during the training period, increased at 3 and 6 weeks of task performance, dropped at 8 wks, but was up regulated again at 12 weeks of task performance compared to normal controls (Fig 1G). Bony trabeculae showed a similar pattern of PLF during the task performance, except that the level at 8 weeks was higher when compared to that in the epiphyseal plate (Fig 1H versus 1G). Results were consistent within each group for these analyses. Periostin, on the other hand, was not detected in the distal epiphyseal plate of radii and ulna between 3 and 12 wks of task performance, but was present at much higher levels in distal trabecular bone compared to PLF (Figs 5A, B; data for weeks 8 and 12 not shown).

Changes in PLF and Periostin levels in distal forearm bone periosteum with task performance

PLF was not detected in the periosteum of radii and ulna from normal control and trained controls animals (Fig 2A, C), but was induced at low levels in these same bones in animals performing the task for three weeks, and greatly increased by 6 and 8 weeks compared to controls (Figs 2D–H). Twelve weeks of task performance resulted in decreased immunostaining of PLF protein in the periosteum compared to 6 and 8 weeks (Fig 2I, J). Quantification of PLF immunoreactivity in the distal diaphyseal periosteum of both the radius and ulna showed highest levels at 6 and 8 wks of task performance compared to normal controls (Fig 3A, the distal diaphyseal periosteum refers to the periosteum at the distal end of the shaft and adjacent to the metaphysis). In the metaphyseal periosteum, PLF was highest at 6 and 8 weeks in the radius and at 6 weeks in the ulna compared to normal controls, suggesting that the two bones are affected differently by task performance (Fig 3B, C). Results were consistent within each group for these analyses. In contrast to the absence of Periostin immunostaining in the distal epiphyseal plate (Fig 5A, B), robust levels of Periostin were observed in the distal periosteum of radii and ulna at all weeks of task performance (Fig 5C, D; data for weeks 3 and 6 not shown). Periostin was not detected in the periosteum of normal control (Fig 5G) or trained control animals (data not shown).

PLF and Periostin levels in the major bone cell types in response to task performance

Bone is formed and remodeled by three major cell types, osteoblasts, osteocytes and osteoclasts. Osteoblasts are responsible for laying down bone matrix, osteocytes support and maintain this matrix, whereas osteoclasts resorb the old bone matrix and make room for new matrix to be laid down. Presence or absence of PLF protein was investigated using immunolocalization techniques in these cell types. PLF was not detected in these cell types in normal control (Fig 4A, B) or trained control animals (data not shown). Although PLF was detected in trabeculae (Figs 1C; 4C) in animals performing the task for 3 weeks, no staining was detected in osteoblasts, osteocytes or osteoclasts (Fig 4C, D). In contrast, PLF was considerably up regulated in all these cell types by 6 and 8 weeks of task performance (Fig 4E–H), but was absent again by 12 weeks of task performance (Fig 4I, J). Results were consistent within each group for these analyses.

A major impact of repetitive task performance is in the forelimb wrist joints [57]. Therefore, we examined PLF localization in the distal articular cartilage of the ulna and radius of the preferred reach limb. Quantification of PLF immunostaining using Bioquant Osteo II software demonstrated a transient pattern of immunoexpression in which PLF was induced at 3 and 6 weeks of task performance compared to normal controls, after which point it decreased back to baseline levels (Fig 4K, L). Periostin was present in osteoblasts and osteocytes (Fig 5E, F) at all times after task performance but remained undetected in the osteoclasts throughout the 12 weeks task performance period (data not shown). Results were consistent within each group for these analyses.

Detection of Periostin by western blot analysis in reach limb bones

Total protein from bones of NC, TC and HRHF (n=3 per group) reach limbs was analyzed by western blot. Periostin was not detected in normal controls, was very low in the trained controls but once induced, levels remained high and unchanged with weeks of task performance (Fig 5G). Results were consistent within each group for the three repetitions of these western blot analyses.

Detection of serum osteocalcin and Trap5b

Serum from NC, TC and HRHF (n=6–8 per group) rats was analyzed using ELISA for a biomarker of bone formation, osteocalcin, and a biomarker of bone resorption, Trap5b. Serum levels of osteocalcin were significantly higher in week 6 HRHF rats compared to normal controls and compared to week 12 HRHF rats (Fig 6A). In contrast, serum levels of Trap5b were significantly higher in week 12 HRHF rats compared to normal controls (Fig 6B).

Morphometry of distal forearm bones of the reach limb

The distal epiphyseal plates of the radius and ulna of the reach limbs of HRHF animals showed epiphyseal plate thinning in week 12, compared to normal control animals (Fig 7A, B). The distal epiphyseal plate of the radius was also thinner in weeks 8 and 12 HRHF rats, compared to trained controls (Fig 7A). The distal cortical wall of the radius and ulna was thinner in the reach limbs of HRHF animals in weeks 8 and 12 compared to normal controls (Fig 7C). In contrast, distal cortical wall of the ulna was thinner in weeks 3, 8 and 12 compared to normal controls, and thinner in weeks 8 and 12 compared to trained control rats (Fig 7D).

Discussion

Bone formation in response to mechanical loading is considered to be a means by which bone adapts to changes in its mechanical environment. An increase in moderate work load (8 reaches/min at <5% MPF) for a short period of time (12 weeks) appears to be beneficial to bone tissue, as it promotes adaptive remodeling in our animal model [53] and in other models in which brief cyclical loading of bone at low magnitude similarly results in anabolic effects [58–61, 63; literature reviewed in detail in 52, 61]. In studies by others, increased osteogenesis was reported in both cancellous and periosteal regions of rat vertebrae after mechanical loading [59, 60]. Also, when rats were run on a treadmill at low intensity and for short durations, their bones adapted by increasing bone mineral density, cortical bone area and stiffness, and by decreasing energy absorbed and twist angle [60]. However, we show here that if work demands are high (12 reaches/min at 60% MPF) and continue for more than 2 months, that apparently the tissues' threshold of adaptive capacity are surpassed and pathological degenerative responses are induced. This agrees with our previous findings in other tissues examining low to high repetition and force paradigms [49, 50, 54, 57]. This also agrees with results from another model in which continued treadmill running at lower magnitudes (90 min/day at a speed of 20 m/min for 9 weeks; 60% VO_2 max) resulted in bone formation [62], while high magnitudes (105 min/day at a speed of 30 m/day for 11 weeks; 80% VO_2 max) resulted in catabolism and microfracture of bones [63]. In these cases of pathological remodeling, bone weakening due to catabolic effects is probably a consequence of constant remodeling and continued loading [64, 65]. In yet another rat model of increased loading, there was an increase in anabolic mRNAs (collagen-1A1, collagen-2A1 and aggrecan) in intervertebral discs at low frequency loading and an increase in catabolic mRNAs (MMP-3, MMP-13 and ADAMTs-4) after high frequency loading [66].

Strategies to improve or alleviate symptoms that result from pathological over load require the identification of molecules that are part of the signaling pathways that mediate these responses. The change in the temporal and spatial pattern of PLF localization over time in our animal model suggested that it might be associated temporally with the adaptive response and thereby worthy of further investigation. The temporal and spatial variation in immunolocalization of PLF to specific regions, tissues and cells within the reach forelimb also suggested that PLF was induced by constant loading of forelimb bones. Furthermore, since PLF was induced in other tissues and organ systems under conditions of stress and

increased load [8, 51, 52], the data presented here may suggest a role for PLF in the early adaptive response to loading.

A low level of induction of PLF was observed in the epiphyseal plate and trabeculae of trained control animals, although at much lower levels than after 3–12 weeks of task performance (PLF was never observed in normal control animals). The 4–6 weeks of initial training at a HRHF level, even for only 10–20 minutes per day, clearly had an effect on distal forearm bones in that levels of PLF increased. These results suggest that there is a training effect in rats learning to perform a high repetition, high demand task that requires the rats to pull at 60% of their maximum grasp force for 10–20 minutes per day, results confirmed in two other studies from our group (57, 68). No training effect has been observed in our previous studies examining the effects of less demanding tasks on musculoskeletal tissues, such as a high repetition low force (HRLF) task [48, 51, 64].

In our rat model, PLF changes occurring at the epiphysis-diaphysis junction by 3 weeks of task performance may be attributed to an increase in compressive load generated across the metaphysis by the combined contraction of both wrist and forepaw flexors and extensors. Similarly, Stokes et al. showed that mechanical loading of tail vertebrae modulated their growth rate, by changing the size of the hypertrophic chondrocytes in the epiphyseal plate [65]. In addition, sustained mechanical load is known to modulate endochondral growth in the immature skeleton, by altering growth rates and numbers of proliferative chondrocytes, their rate of proliferation, and the amount of chondrocytic enlargement occurring in the hypertrophic zone [66]. PLF is present in chondrocytes during skeletal embryonic development [56]. Therefore, in our rat model, it may be induced in response to loading in the epiphyseal plate, although an adaptive response is of course limited in epiphyseal plates of young adult rats. Our observed increase of PLF in week 6 in all bone regions examined coincided temporally with an increase in serum osteocalcin, a biomarker of bone formation. Also, our observed decrease in PLF in week 12 in the periosteum and metaphyseal regions coincided temporally with an increase in serum TRAP5b, a biomarker of bone resorption. This decrease in PLF also coincided temporally with thinning of the distal epiphyseal plates and cortical walls, the latter change also suggestive of bone resorption. These results support our hypothesis that PLF is associated with anabolic bone changes between weeks 3 and 6 of task performance. Interestingly, its spatial location in the epiphyseal plate and trabeculae at 12 weeks of task performance, where it increased again after a decrease at 8 weeks, was very different than at 3 and 6. In week 12, it was no longer intracellular, but only within the matrix surrounding hypertrophied chondrocytes. This latter finding suggests that PLF may also be involved in catabolic events, although longer periods of task performance are needed to explore this question.

In addition, PLF was also detected in the cellular layer of the periosteum at 3 – 8 weeks of task performance, but not at 12 weeks. It was never detected in the periosteum of normal or trained control animals over the 12 weeks of task performance. Since the cellular layer of the periosteum contains osteoblast progenitor cells, we interpret localization to this layer to mean that PLF is playing an anabolic role. This hypothesis is supported by our recent findings that PLF promotes bone formation *in vivo* and *in vitro* [44]. The recruitment of periosteal stem cells to the osteogenic lineage is not well studied. Thus, it would be interesting to determine if PLF plays a role in this regard. As to the absence of PLF in the periosteum in week 12, we suggest that this may be explained by the presence of a pathologic inflammatory response in week 12 in which periosteal bone resorption and degradation far exceed bone anabolic events due to continued task performance [51, 54, 57].

PLF was also highly induced by 6 and 8 weeks of task performance in osteoblasts, osteocytes, and osteoclasts, cells involved in remodeling, further suggesting a role for PLF

in the adaptive remodeling process of bone. At 6 and 8 weeks of task performance, PLF was clearly present in both flattened as well as in cubodial osteoblasts lining cortical and trabecular bone. This difference in osteoblast phenotype is routinely used to classify them as inactive (flattened) or active (cubodial). After mechanical stimulation, trabecular bone surface cells (flattened) develop ultrastructural features of osteoblast differentiation and activity. They acquire a cuboidal shape with abundant rough endoplasmic reticulum and rounded nuclei, which correlate temporally with bone matrix production [69]. Together these data support our idea that PLF has an anabolic role in promoting bone formation, possibly by increasing proliferation and differentiation of osteoblasts [44] or by recruiting osteoblast progenitor cells to the osteogenic lineage. In addition, PLF appears to be located in the nuclei of bone cells (Fig. 4G), a finding that correlates with PLF having a nuclear localization signal [9]. Interestingly, PLF expression in these cell types is absent by 12 weeks of HRHF task performance, a time when adaptive remodeling has given way to frank inflammation and degeneration [57]. Significant inflammation and an increase in activated osteoclasts were also observed in our previous studies examining the effects of lower demand tasks on bone tissues [51, 54, 55].

Periostin was not detected in normal control animals but was induced at low levels in trained control animals. However, unlike PLF, once Periostin was induced by task performance, it continued to be present at a uniformly high level. Because it was constitutively expressed at high levels in the periosteum, trabeculae and bone forming and resorbing cells, the level of Periostin was not quantified by Bioquant Osteo II. Since others have shown that Periostin is produced by fibroblasts, we expected to see it localized to both the inner and outer layers of the periosteum. Its presence throughout the periosteum after induction suggests that it plays a role as a matrix protein [43]. Since ostocytes are known to produce bone matrix proteins and respond to bone loading [67], we suggest that the staining observed in osteocytes is in response to loading. Unlike PLF, Periostin was not detected between weeks 3 and 12 in the epiphyseal plate or in osteoclasts. However, it was always present at high levels in trabecular bone, again suggesting that it is a matrix protein. This variation in the spatial pattern of immunolocalization of Periostin versus PLF suggests that even though they are single gene products of alternatively spliced mRNAs, they respond to loading differently. The differences in the spatial and temporal location of the two isoforms also suggest that they have different roles in tissue remodeling. We hypothesize that PLF might be a marker of early adaptive remodeling to repetitive overloading while Periostin may be involved in matrix deposition after repetitive loading.

In summary, PLF is present primarily in the periosteum, articular cartilage, metaphyses', and osteoblasts, osteocytes and osteoclasts during the adaptive phase of remodeling in WMSD. In general, the data on these tissues suggest that the pattern of PLF localization varies considerably; both in space and time so that it is located in tissues in the early stage of bone loading but disappear once tissues are in the pathological phase of response. In addition, since the level of PLF peaks at 6 weeks of HRHF task performance in bone, a time point associated with increased serum osteocalcin, but down regulates thereafter, we suggest that it may be a tissue marker of adaptive bone remodeling. In contrast, since Periostin does not alter its expression pattern across weeks of task performance, it serves instead as a marker of constant high loading.

References

1. Zinn K, McAllister L, Goodman CS. Sequence analysis and neuronal expression of fasciclin I in grasshopper and Drosophila. Cell. 1988; 53(4):577–587. [PubMed: 3370670]
2. Litvin J, Zhu S, Norris R, Markwald R. The periostin family of proteins: therapeutic targets for heart disease. Anat Rec. 2005; 287(2):1205–12.

3. Coutu DL, Wu JH, Monette A, Rivard GE, Blostein MD, Galipeau J. Periostin, a member of a novel family of vitamin K-dependent proteins, is expressed by mesenchymal stromal cells. J Biol Chem. 2008 Jun 27; 283(26):17991–8001. Epub 2008 Apr 30. [PubMed: 18450759]
4. Huber O, Sumper M. Algal-CAMs: isoforms of a cell adhesion molecule in embryos of the alga Volvox with homology to Drosophila fasciclin I. EMBO J. 1994; 18:4212–4222. [PubMed: 7925267]
5. Terasaka K, Yamaguchi R, Matsuo K, Yamazaki A, Nagai S, Yamada T. Complete nucleotide sequence of immunogenic protein MPB70 from Mycobacterium bovis. BCG, FEMS Microbiol Lett. 1989; 49:2–3. 273–276.
6. Politz O, Gratchev A, McCourt PA, Schledzewski K, Guillot P, Johansson S, Svineng G, Franke P, Kannicht C, Kzhyshkowska J, Longati P, Velten FW, Johansson S, Goerdt S. Stabilin-1 and -2 constitute a novel family of fasciclin-like hyaluronan receptor homologues. Biochem J 362. 2002; 1:155–164. [PubMed: 11829752]
7. Skonier J, Neubauer M, Madisen L, Bennett K, Plowman GD, Purchio AF. CDNA cloning and sequence analysis of βig-h3, a novel gene induced in a human adenocarcinoma cell line after treatment with transforming growth factor-beta. DNA Cell Biol. 1992; 11:511–522. [PubMed: 1388724]
8. Horiuchi K, Amizuka N, Takeshita S, Takamatsu H, Katsuura M, Ozawa H, Toyama Y, Bonewald LF, Kudo. Identification and characterization of a novel protein, Periostin, with restricted expression to periosteum and periodontal ligament and increased expression by transforming growth factor beta. J Bone Miner Res. 1999; 14:1239–1249. [PubMed: 10404027]
9. Litvin J, Selim A, Montgomery M, Lehmann K, Devlin H, Bednarik D, Safadi F. Expression and function of periostin-isoforms in bone. J Biol Chem. 2004; 92:1044–1061.
10. Katsuragi N, Morishita R, Nakamura N, Ochiai T, Taniyama Y, Hasegawa Y, Kawashima K, Kaneda Y, Ogihara T, Sugimura K. Periostin as a novel factor responsible for ventricular dilation. Circulation. 2004; 110:1806–1813. [PubMed: 15381649]
11. Kii I, Amizuka N, Minqi L, Kitajima S, Saga Y, Kudo A. Periostin is an extracellular matrix protein required for eruption of incisors in mice. Biochem Biophys Res Commun. 2006; 342:766–772. [PubMed: 16497272]
12. Kruzynska-Frejtag A, Wang J, Maeda M, Rogers R, Krug E, Hoffman S, Markwald RR, Conway SJl. Periostin is expressed within the developing teeth at the sites of epithelial–mesenchymal interaction. Dev Dyn. 2004; 229:857–868. [PubMed: 15042709]
13. Lallier TE, Spencer A. Use of microarrays to find novel regulators of periodontal ligament fibroblast differentiation. Cell Tissue Res. 2007; 327:93–109. [PubMed: 17024420]
14. Suzuki H, Amizuka N, Kii I, Kawano Y, Nozawa-Inoue K, Suzuki A, Yoshie H, Kudo A, Maeda T. Immunohistochemical localization of periostin in tooth and its surrounding tissues in mouse mandibles during development. Anat Rec A Discov Mol Cell Evol Biol. 2004; 281:1264–1275. [PubMed: 15386274]
15. Kruzynska-Frejtag A, Machnicki M, Rogers R, Markwald RR, Conway SJ. Periostin (an osteoblast specific factor) is expressed within the embryonic mouse heart during valve formation. Mech Dev. 2001; 103:183–188. [PubMed: 11335131]
16. Norris RA, Kern CB, Wessels A, Moralez EI, Markwald RR, Mjaatvedt CH. Identification and detection of the periostin gene in cardiac development. Anat Rec A Discov Mol Cell Evol Biol. 2004; 281(2):1227–33. [PubMed: 15532025]
17. Norris RA, Kern CB, Wessels A, Wirrig EE, Markwald RR, Mjaatvedt CH. Detection of betaig-H3, a TGFbeta induced gene, during cardiac development and its complementary pattern with periostin. Anat Embryol (Berl). 2005; 210(1):13–23. [PubMed: 16034610]
18. Kern CB, Hoffman S, Moreno R, Damon BJ, Norris RA, Krug EL, Markwald RR, Mjaatvedt CH. Immunolocalization of chick periostin protein in the developing heart. Anat Rec A Discov Mol Cell Evol Biol. 2005; 284:415–423. [PubMed: 15803479]
19. Lindsley A, Li W, Wang J, Maeda N, Rogers R, Conway SJ. Comparison of the four mouse fasciclin-containing genes expression patterns during valvuloseptal morphogenesis. Gene Expr Patterns. 2005; 5:593–600. [PubMed: 15907457]

20. Litvin J, Blagg A, Mu A, Matiwala S, Montgomery M, Berretta R, Houser S, Margulies K. Periostin and Periostin-like factor in the human heart: possible therapeutic targets. Cardiovasc Pathol. 2006; 15(1):24–32. [PubMed: 16414453]
21. Litvin J, Chen X, Keleman S, Zhu S, Autieri M. Expression and function of periostin-like factor in vascular smooth muscle cells. Am J Physiol Cell Physiol. 2007 May; 292(5):C1672–80. Epub 2006 Nov 8. [PubMed: 17092992]
22. Lindner V, Wang Q, Conley BA, Friesel RE, Vary CP. Vascular injury induces expression of periostin: implications for vascular cell differentiation and migration. Arterioscler Thromb Vasc Biol. 2005; 25:77–83. [PubMed: 15514205]
23. Stanton LW, Garrard LJ, Damm D, Garrick BL, Lam A, Kapoun AM, Zheng Q, Protter AA, Schreiner GF, White RT. Altered patterns of gene expression in response to myocardial infarction. Circ Res. 2000; 86:939–934. [PubMed: 10807865]
24. Wang D, Oparil S, Feng JA, Li P, Perry G, Chen LB, Dai M, John SW, Chen YF. Effects of pressure overload on extracellular matrix expression in the heart of the atrial natriuretic peptide-null mouse. Hypertension. 2003; 42:88–95. [PubMed: 12756220]
25. Choi P, Jordan CD, Mendez E, Houck J, Yueh B, Farwell DG, Futran N, Chen C. Examination of oral cancer biomarkers by tissue microarray analysis. Arch Otolaryngol Head Neck Surg. 2008; 34(5):539–46. [PubMed: 18490578]
26. Fukushima N, Kikuchi Y, Nishiyama T, Kudo A, Fukayama M. Periostin deposition in the stroma of invasive and intraductal neoplasms of the pancreas. Mod Pathol. 2008; 21(8):1044–53. [PubMed: 18487994]
27. Kudo Y, Ogawa I, Kitajima S, Kitagawa M, Kawai H, Gaffney PM, Miyauchi M, Takata T. Periostin promotes invasion and anchorage-independent growth in the metastatic process of head and neck cancer. Cancer Res. 2006; 66(14):6928–35. [PubMed: 16849536]
28. Sasaki H, Auclair D, Kaji M, Fukai I, Kiriyama M, Yamakawa Y, Fujii Y, Chen LB. Serum level of the periostin, a homologue of an insect cell adhesion molecule, in thymoma patients. Cancer Lett. 2001; 172:37–34. [PubMed: 11595127]
29. Crnogorac-Jurcevic T, Missiaglia E, Blaveri E, Gangeswaran R, Jones M, Terris B, Costello E, Neoptolemos JP, Lemoine NR. Molecular alterations in pancreatic carcinoma: expression profiling shows that dysregulated expression of S100 genes is highly prevalent. J Pathol. 2003; 201(1):63–74. [PubMed: 12950018]
30. Tilman G, Mattiussi M, Brasseur F, van Baren N, Decottignies A. Human periostin gene expression in normal tissues, tumors and melanoma: evidences for Periostin production by both stromal and melanoma cells. Mol Cancer. 2007; 17(6):80. [PubMed: 18086302]
31. Lal A, Lash AE, Altschul SF, Velculescu V, Zhang L, McLendon RE, Marra MA, Prange C, Morin PJ, Polyak K, Papadopoulos N, Vogelstein B, Kinzler KW, Strausberg RL, Riggins GJ. A public database for gene expression in human cancers. Cancer Res. 1999; 59(21):5403–5407. [PubMed: 10554005]
32. Sasaki H, Yu CY, Dai M, Tam C, Loda M, Auclair D, Chen LB, Elias A. Elevated serum periostin levels in patients with bone metastases from breast but not lung cancer. Breast Cancer Res Treat. 2003; 77(3):245–52. [PubMed: 12602924]
33. Shao R, Bao S, Bai X, Blanchette C, Anderson RM, Dang T, Gishizky ML, Marks JR, Wang XF. Acquired expression of periostin by human breast cancers promotes tumor angiogenesis through up-regulation of vascular endothelial growth factor receptor 2 expression. Mol Cell Biol. 2004; 24(9):3992–4003. [PubMed: 15082792]
34. Puglisi F, Puppin C, Pegolo E, Andreetta C, Pascoletti G, D'Aurizio F, Pandolfi M, Fasola G, Piga A, Damante G, Di Loreto C. Expression of periostin in human breast cancer. J Clin Pathol. 2008; 61(4):494–8. [PubMed: 17938160]
35. Sasaki H, Auclair D, Fukai I, Kiriyama M, Yamakawa Y, Fujii Y, Chen LB. Serum level of the periostin, a homologue of an insect cell adhesion molecule, as a prognostic marker in non-small cell lung carcinomas. Cancer. 2001; 92(4):843–8. [PubMed: 11550156]
36. Matei D, Graeber TG, Baldwin RL, Karlan BY, Rao J, Chang DD. Gene expression in epithelial ovarian carcinoma. Oncogene. 2002; 21(41):6289–98. [PubMed: 12214269]

37. Bao S, Ouyang G, Bai X, Huang Z, Ma C, Liu M, Shao R, Anderson RM, Rich JN, Wang XF. Periostin potently promotes metastatic growth of colon cancer by augmenting cell survival via the Akt/PKB pathway. Cancer Cell. 2004; 5(4):329–39. [PubMed: 15093540]
38. Kikuchi Y, Kashima TG, Nishiyama T, Shimazu K, Morishita Y, Shimazaki M, Kii I, Horie H, Nagai H, Kudo A, Fukayama M. Periostin is expressed in pericryptal fibroblasts and cancer-associated fibroblasts in the colon. J Histochem Cytochem. 2008; 56(8):753–64. [PubMed: 18443362]
39. Yoshioka N, Fuji S, Shimakage M, Kodama K, Hakura A, Yutsudo M, Inoue H, Nojima H. Suppression of anchorage-independent growth of human cancer cell lines by the TRIF52/periostin/OSF-2 gene. Exp Cell Res. 2002; 279(1):91–99. [PubMed: 12213217]
40. Erkan M, Kleeff J, Gorbachevski A, Reiser C, Mitkus T, Esposito I, Giese T, Büchler MW, Giese NA, Friess H. Periostin creates a tumor-supportive microenvironment in the pancreas by sustaining fibrogenic stellate cell activity. Gastroenterology. 2007; 132(4):1447–64. [PubMed: 17408641]
41. Oku E, Kanaji T, Takata Y, Oshima K, Seki R, Morishige S, Imamura R, Ohtsubo K, Hashiguchi M, Osaki K, Yakushiji K, Yoshimoto K, Ogata H, Hamada H, Izuhara K, Sata M, Okamura T. Periostin and bone marrow fibrosis. Int J Hematol. 2008; 88(1):57–63. [PubMed: 18465194]
42. Takayama G, Arima K, Kanaji T, Toda S, Tanaka H, Shoji S, McKenzie AN, Nagai H, Hotokebuchi T, Izuhara K. Periostin: a novel component of subepithelial fibrosis of bronchial asthma downstream of IL-4 and IL-13 signals. J Allergy Clin Immunol. 2006; 118(1):98–104. [PubMed: 16815144]
43. Norris RA, Damon B, Mironov V, Kasyanov V, Ramamurthi A, Moreno-Rodriguez R, Trusk T, Potts JD, Goodwin RL, Davis J, Hoffman S, Wen X, Sugi Y, Kern CB, Mjaatvedt CH, Turner DK, Oka T, Conway SJ, Molkentin JD, Forgacs G, Markwald RR. Periostin regulates collagen fibrillogenesis and the biomechanical properties of connective tissues. J Cell Biochem. 2007; 101(3):695–711. [PubMed: 17226767]
44. Zhu S, Barbe MF, Liu C, Hadjiargyrou M, Popoff SN, Rani S, Safadi FF, Litivn J. Periostin-like-factor in Osteogenesis. Journal of Cellular Physiology. 2008 In Press. J Cell Physiol.
45. Bureau of Labor Statistics. Lost-work time injuries and illnesses: characteristics and resulting, days away from work. United States Department of Labor News USDL. Mar 30.2005 :05–521.
46. Bernard. Musculoskeletal Disorders (MSDs) and Workplace factors: A Critical Review of Epidemiological Evidence for Work-related Musculoskeletal Disorders of the Neck, Upper Extremity, and Low Back. Bernard, BP., editor. U.S. Department of Health and Human Services, Public Health Service, Centers for Disease Control. National Institute for Occupational Safety and Health; Cincinnati, OH: 1997. Publication no. 97–141
47. National Research Council and Institute of Medicine. Musculoskeletal Disorders and the Workplace. National Academy Press; Washington, DC: 2001. p. 57-59.
48. Barbe MF, Barr AE, Gorzelany I, Amin M, Gaughan JP, Safadi FF. Chronic repetitive reaching and grasping results in decreased motor performance and widespread tissue responses in a rat model of MSD. J Orthop Res. 2003; 21:167–176. [PubMed: 12507595]
49. Clark BD, Al-Shatti T, Barr AE, Amin M, Barbe MF. Performance of a high-repetition, high-force task induces carpel tunnel syndrome in rats. J Orthop Sports Phys Ther. 2004; 34:244–253. [PubMed: 15189016]
50. Clark BD, Barr AE, Safadi FF, Beitman L, Al-Shatti T, Amin M, Gaughan JP, Barbe MF. Median nerve trauma in a rat model of work-related musculoskeletal disorder. J Neurotrauma. 2003; 20:681–695. [PubMed: 12908929]
51. Barr AE, Safadi FF, Gorzelany I, Amin M, Popoff SN, Barbe MF. Repetitive, negligible force reaching in rats induces pathological overloading of upper extremity bones. J Bone Miner Res. 2003; 18(11):2023–32. [PubMed: 14606516]
52. Barr AE, Barbe MF, Clark BD. Systemic inflammatory mediators contribute to widespread effects in work-related musculoskeletal disorders. Exerc Sport Sci Rev. 2004; 32(4):135–42. [PubMed: 15604931]

53. Al-Shatti T, Barr AE, Safadi FF, Amin M, Barbe MF. Increase in inflammatory cytokines in median nerves in a rat model of repetitive motion injury. J Neuroimmunol. 2005; 167(1–2):13–22. [PubMed: 16026858]
54. Barbe MF, Elliott MB, Abdelmagid SM, Amin M, Popoff SN, Safadi FF, Barr AE. Serum and tissue cytokines and chemokines increase with repetitive upper extremity tasks. J Orthop Res. 2008; 26:1320–1326. [PubMed: 18464247]
55. Elliott MB, Barr AE, Kietrys DM, Al-Shatti T, Amin M, Barbe MF. Peripheral neuritis and increased spinal cord neurochemicals are induced in a model of repetitive motion injury with low force and repetition exposure. Brain Res. 2008; 1218:103–13. [PubMed: 18511022]
56. Zhu S, Barbe MF, Amin N, Rani S, Popoff SN, Safadi FF, Litvin J. Immunolocalization of Periostin-like factor and Periostin during embryogenesis. J Histochem Cytochem. 2008; 56(4): 329–45. [PubMed: 18040074]
57. Driban JB, Barr AE, Amin M, Sitler MR, Ziskin M, Kendrick ZV, Barbe MF. A novel model for inducing joint inflammation and degeneration with a pharmacological intervention to reduce its effects. Osteoarthritis and Cartilage. 2008 Submitted.
58. Chow JW, Jagger CJ, Chambers TJ. Characterization of osteogenic response to mechanical stimulation in cancellous bone of rat caudal vertebrae. Am J Physiol. 1993; 265(2 Pt 1):E340–7. [PubMed: 8368304]
59. Chambers TJ, Evans M, Gardner TN, Turner-Smith A, Chow JW. Induction of bone formation in rat tail vertebrae by mechanical loading. Bone Miner. 1993; 20(2):167–78. [PubMed: 8453332]
60. Wheeler DL, Graves JE, Miller GJ, Vander Griend RE, Wronski TJ, Powers SK, Park HM. Effects of running on the torsional strength, morphometry, and bone mass of the rat skeleton. Med Sci Sports Exerc. 1995; 27(4):520–9. [PubMed: 7791582]
61. Barr AE, Barbe MF. Pathophysiological tissue changes associated with repetitive movement: a review of the evidence. Phys Ther. 2002 Feb; 82(2):173–87. Review. [PubMed: 11856068]
62. Bourrin S, Palle S, Pupier R, Vico L, Alexandre C. Effect of physical training on bone adaptation in three zones of the rat tibia. J Bone Miner Res. 1995 Nov; 10(11):1745–52. [PubMed: 8592952]
63. Bourrin S, Genty C, Palle S, Gharib C, Alexandre C. Adverse effects of strenuous exercise: a densitometric and histomorphometric study in the rat. J Appl Physiol. 1994; 76(5):1999–2005. [PubMed: 8063662]
64. Maclean JJ, Lee CR, Alini M, Iatridis JC. Anabolic and catabolic mRNA levels of the intervertebral disc vary with the magnitude and frequency of in vivo dynamic compression. J Orthop Res. 2004; 22(6):1193–200. [PubMed: 15475197]
65. Stokes IA. Mechanical effects on skeletal growth. J Musculoskelet Neuronal Interact. 2002; 2(3): 277–80. [PubMed: 15758453]
66. Stokes IA, Clark KC, Farnum CE, Aronsson DD. Alterations in the growth plate associated with growth modulation by sustained compression or distraction. Bone. 2007; 41(2):197–205. [PubMed: 17532281]
67. Colopy SA, Benz-Dean J, Barrett JG, Sample SJ, Lu Y, Danova NA, Kalscheur VL, Vanderby R Jr, Markel MD, Muir P. Response of the osteocyte syncytium adjacent to and distant from linear microcracks during adaptation to cyclic fatigue loading. Bone. 2004 Oct; 35(4):881–91. [PubMed: 15454095]
68. Albrecht PJ, Thachara A, Vickers J, Barne MF, Barr AE, Rice FL. Alterations in cutaneous innervation and epidermal chemistry following repetitive motion injury in rats. Society for Neuroscience. 2008 Poster Number 154.6.

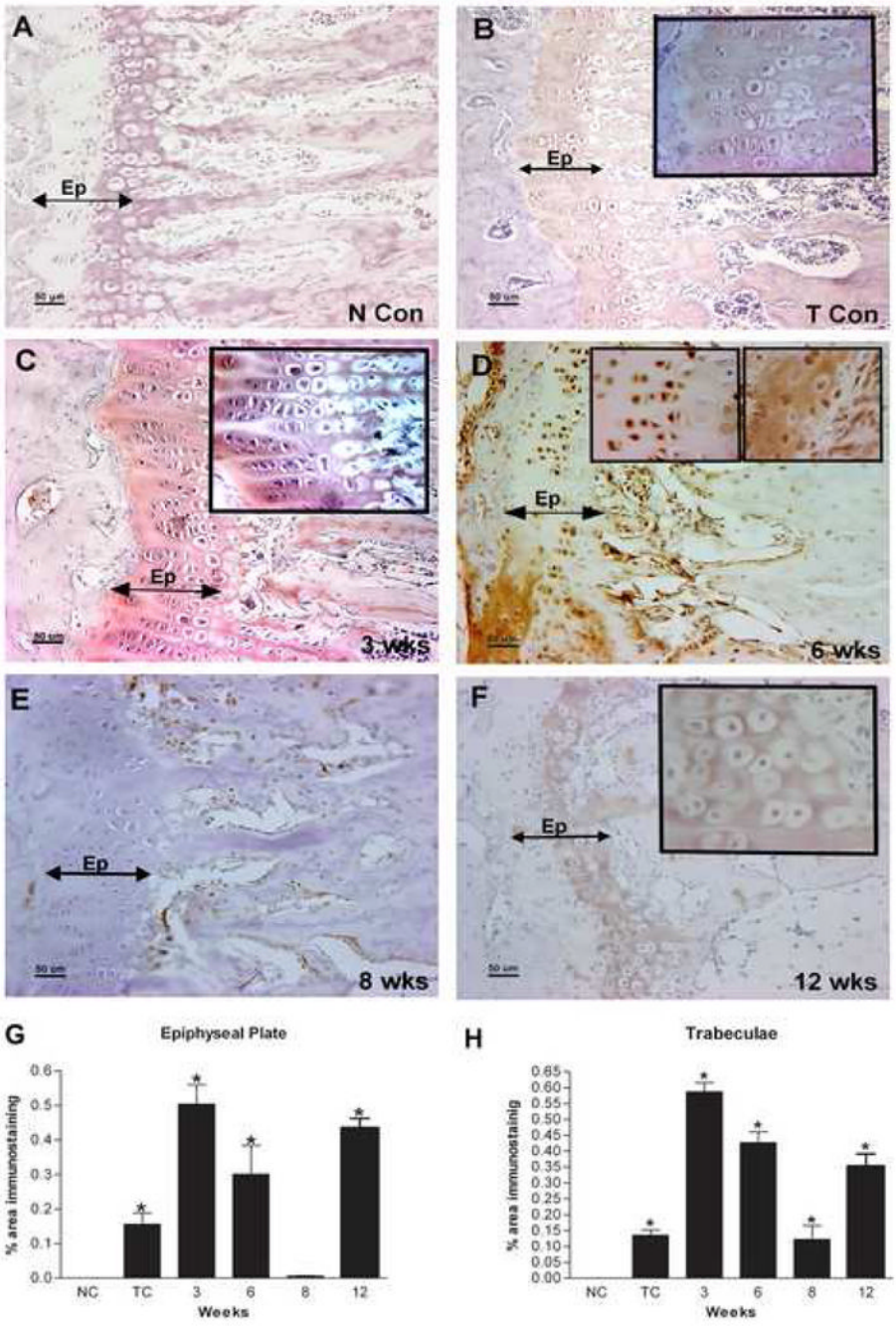

Figure 1.

A–F: Immunolocalization of PLF in the forelimb epiphyseal plate of radii and ulna of normal control (N Con), Trained control (T Con), or HRHF task (3, 6, 8, and 12 wks) animals. Forelimb bone sections were immunoreacted with PLF antibody (brown color indicates positive staining) and counterstained with haematoxylin (a nuclear stain). PLF was (**A**) not detected in bones of N Con animals as indicated by the lack of brown color, but (**B**) was detected at low levels in T Con animals in trabeculae and in proliferating, prehypertrophy, and hypertrophy zones of the epiphyseal plate (inset: cells in the epiphyseal plate shown at higher magnification, staining detected in the matrix surrounding cells). (**C**) PLF was detected at 3 wks in trabeculae and proliferating, prehypertrophy, and hypertrophy

zones in the epiphyseal plate, and (**D**) at 6 wks in the nuclei of prehypertrophy chondrocytes (left and right inset), and in the matrix around hypertrophied chondrocytes (right inset) in the epiphyseal plate. (**E**) PLF was not detected at 8 wks in the epiphyseal plate, but (**F**) was detected at 12 wks in hypertrophied chondrocytes in the epiphyseal plate (inset). **G–H**: PLF levels in the epiphyseal plate (**G**) and trabeculae (**H**) was quantified using a microscope interfaced with an image analysis system (Bioquant Osteo II) and plotted as percent area of PLF immunostaining against weeks of task performance. **Ep**=epiphyseal plate, NCon/**NC** = normal control, **Tb**=trabeculae, **TC** = trained control.

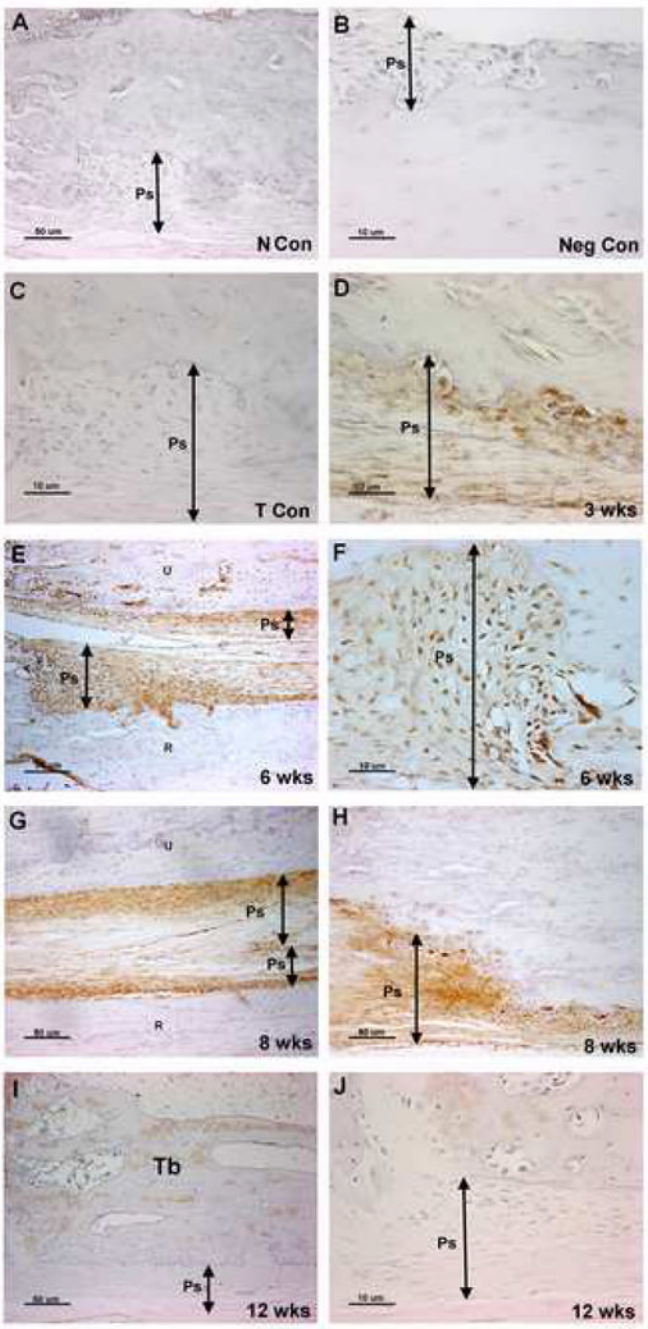

Figure 2.

A–J: Immunolocalization of PLF in the distal diaphyses and periosteum of radii and ulna of normal control (N Con), trained control (T Con), and HRHF (3, 6, 8, and 12 wks) animals. Forelimb bone sections were immunoreacted with PLF antibody (brown color) and counterstained with haematoxylin. PLF was (**A**) not detected in the periosteum of N Con, (**B**) not detected in a HRHF negative staining control, in which primary antibody was omitted, (**C**) not detected in T Con, (**D**) detected at low levels at 3 wks **(E**, **F**) detected at high levels at 6 wks, (**G, H**) and detected at high levels at 8 wks. (**I, J)** PLF was not detected

at 12 wks. **Ps**=Periosteum, **NCon** = normal control, **Tb**=trabeculae, **TCon** = trained control, **Neg Con**= Negative (no antibody) control.

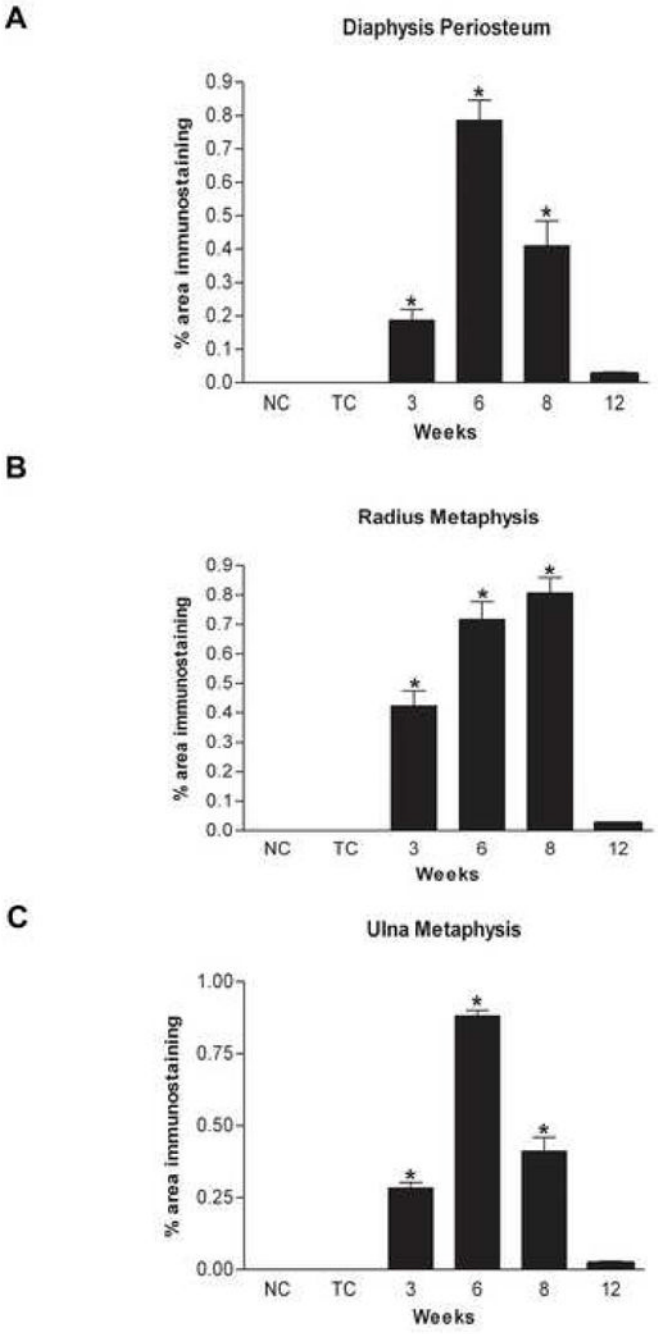

Figure 3.

A–C: PLF levels determined by immunolocalization were quantified by Bioquant Osteo II in the (**A**) distal diaphyseal periosteum of radii and ulna, (**B**) radius metaphyseal junction and (**C**) ulna metaphyseal junction of bones and plotted as PLF immunoexpression against weeks of HRHF task performance. **NC** = normal control, **TC** = trained control.

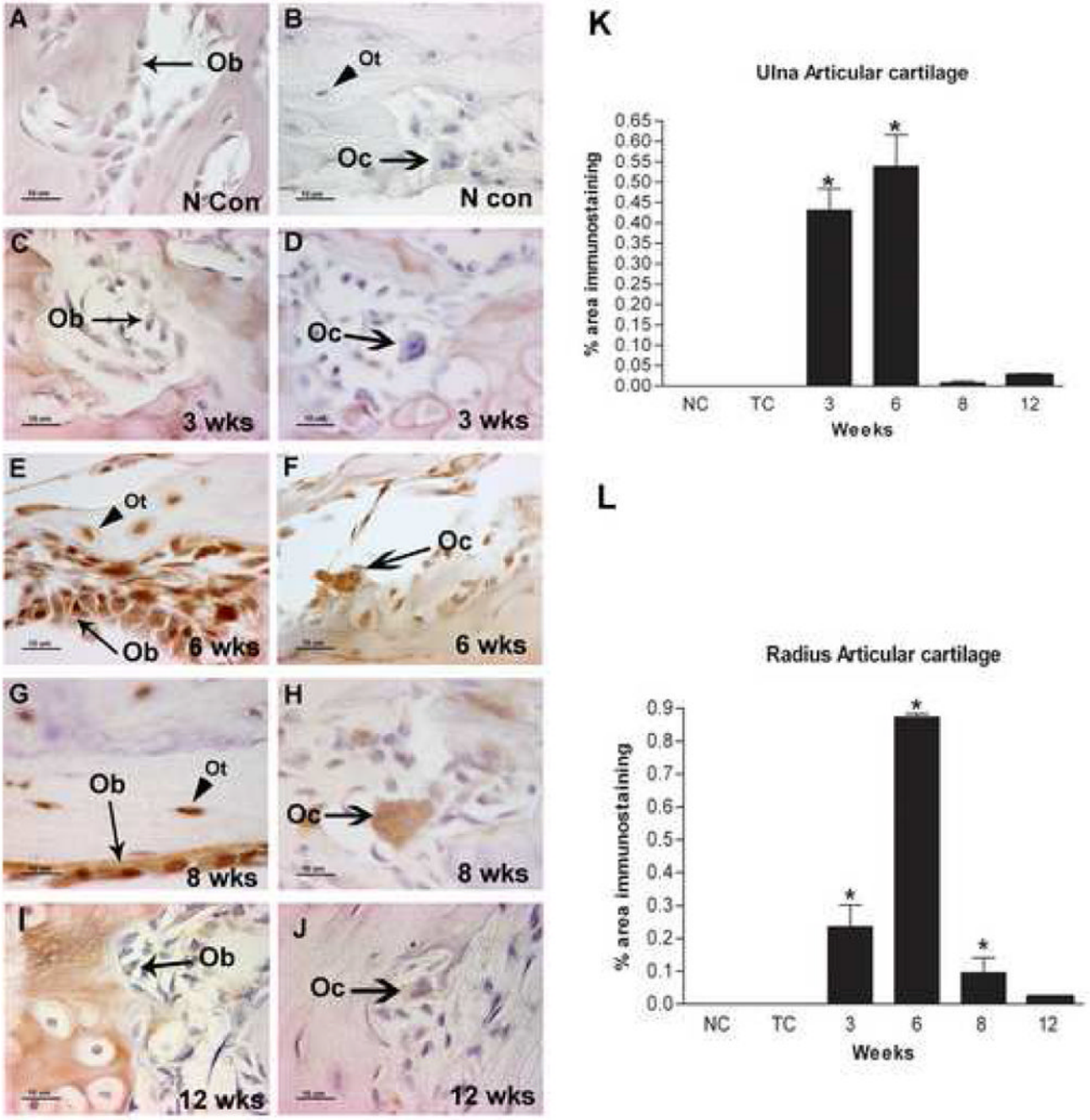

Figure 4.

A–J: Localization of PLF in the osteoblasts, osteoclasts and osteocytes of normal control (N con) or HRHF (3, 6, 8, and 12 wks) animals. Forelimb bone sections were immunoreacted with PLF antibody (brown color) and counterstained with hematoxylin. No PLF was detected in osteoblasts (**A**), osteoclasts or osteocytes (**B, C, D**) in normal control or 3 wks HRHF animals. Animals that performed the task for 6 and 8 weeks had robust expression of PLF in osteoblasts and osteocytes (**E, G**) and in osteoclasts (**F, H**). PLF was down regulated in these cell types in 12 HRHF rats (**I, J**). **K–L**: PLF levels in distal ulna **(K)** and radius articular cartilage (**L**) was quantified using a microscope interfaced with an image analysis

system (Bioquant Osteo II) and plotted as PLF immunostaining against weeks of task performance. **Ob=**osteoblast, **Oc=**osteoclast, **Ot=**osteocyte, **N Con/NC** = normal control, **TC** = trained control.

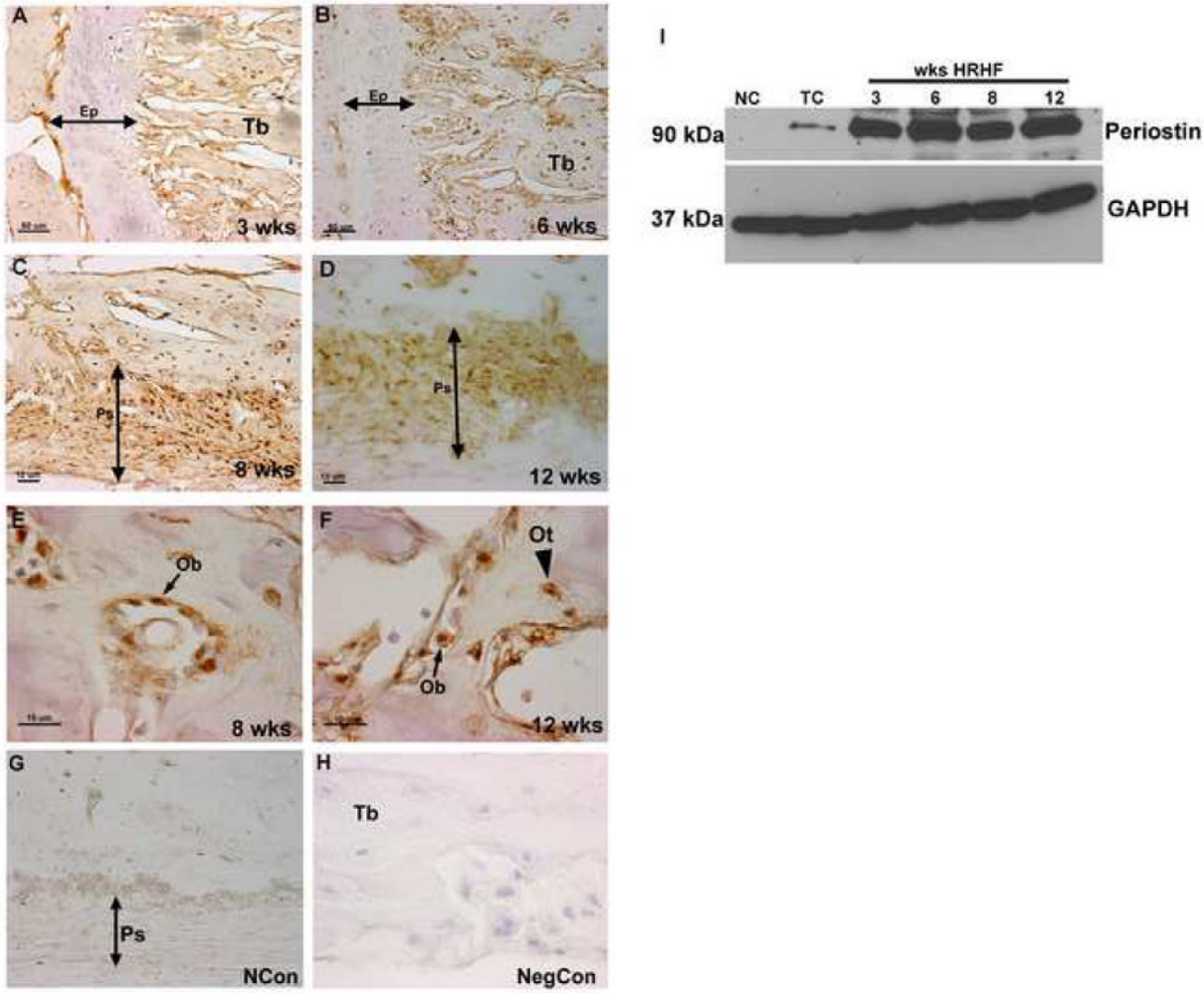

Figure 5.

A–I Immunolocalization of Periostin in the epiphyseal plate and periosteum and in osteoblasts and osteocytes of HRHF rats (3, 6, 8, and 12 wks). Forelimb bone sections (radii and ulna) were immunoreacted with Periostin antibody (brown color) and counterstained with haematoxylin. Periostin was detected in the periosteum, osteoblasts and osteocytes at all time points, but was not detected in the epiphyseal plate. Representative data for epiphyseal plate at 3 and 6 wks (**A**, **B**), periosteum at 8 and 12 wks (**C, D**), and osteoblasts and osteocytes at 8 and 12 wks (**E**, **F).** Normal control (NCon) section reacted with anti-Periostin (**G**) and negative control (NegCon; no primary antibody, **H**). Detection of Periostin by western blot analysis (**I**). **Ep**=epiphyseal plate, **Ps**=periosteum, **Tb**=trabeculae, **Ob**=osteoblast, **Ot**=osteocyte.

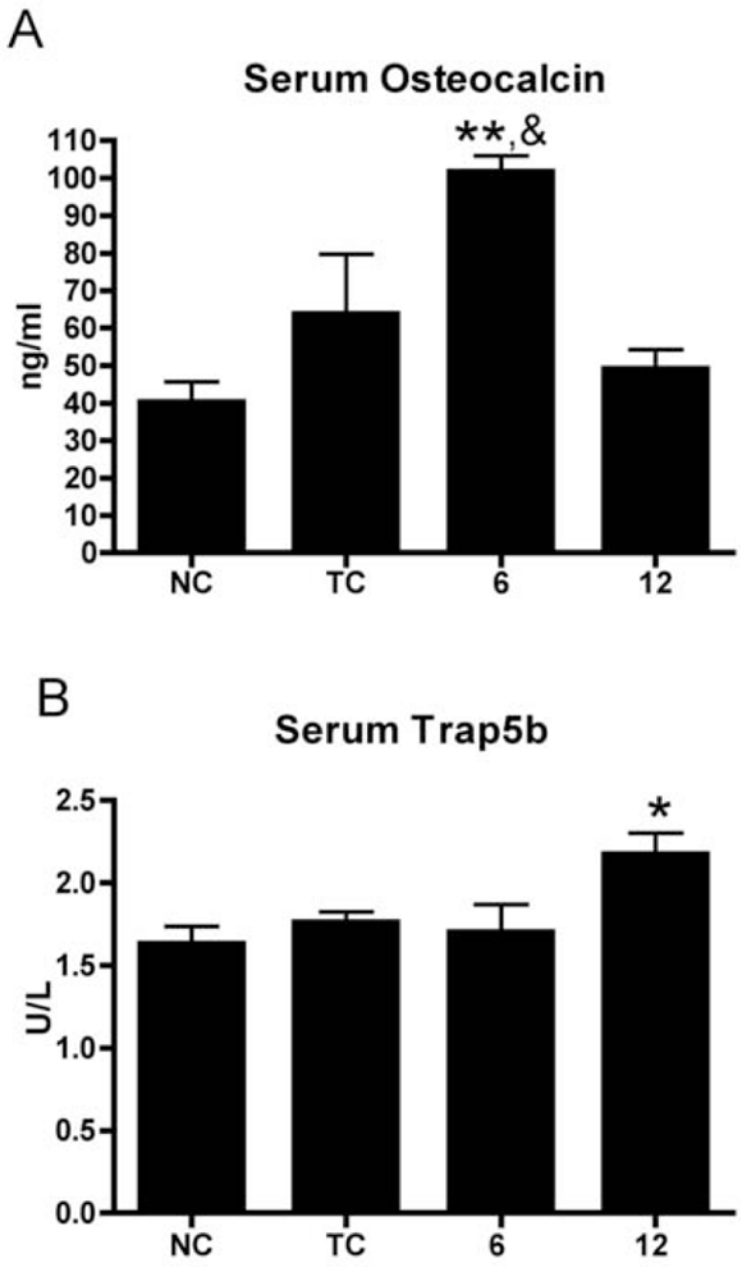

Figure 6.

ELISA detection of serum levels of osteocalcin and Trap5b in normal control (NC), trained control (TC), and HRHF (6 and 12 wk) animals. (**A**) Serum osteocalcin was increased significantly in week 6 HRHF animals compared to normal controls (**: $p<0.001$) and compared to week 12 HRHF rats (&: $p<0.05$). (**B**) Serum Trap5b was increased significantly in week 12 HRHF animals compared to normal controls (*: $p<0.05$).

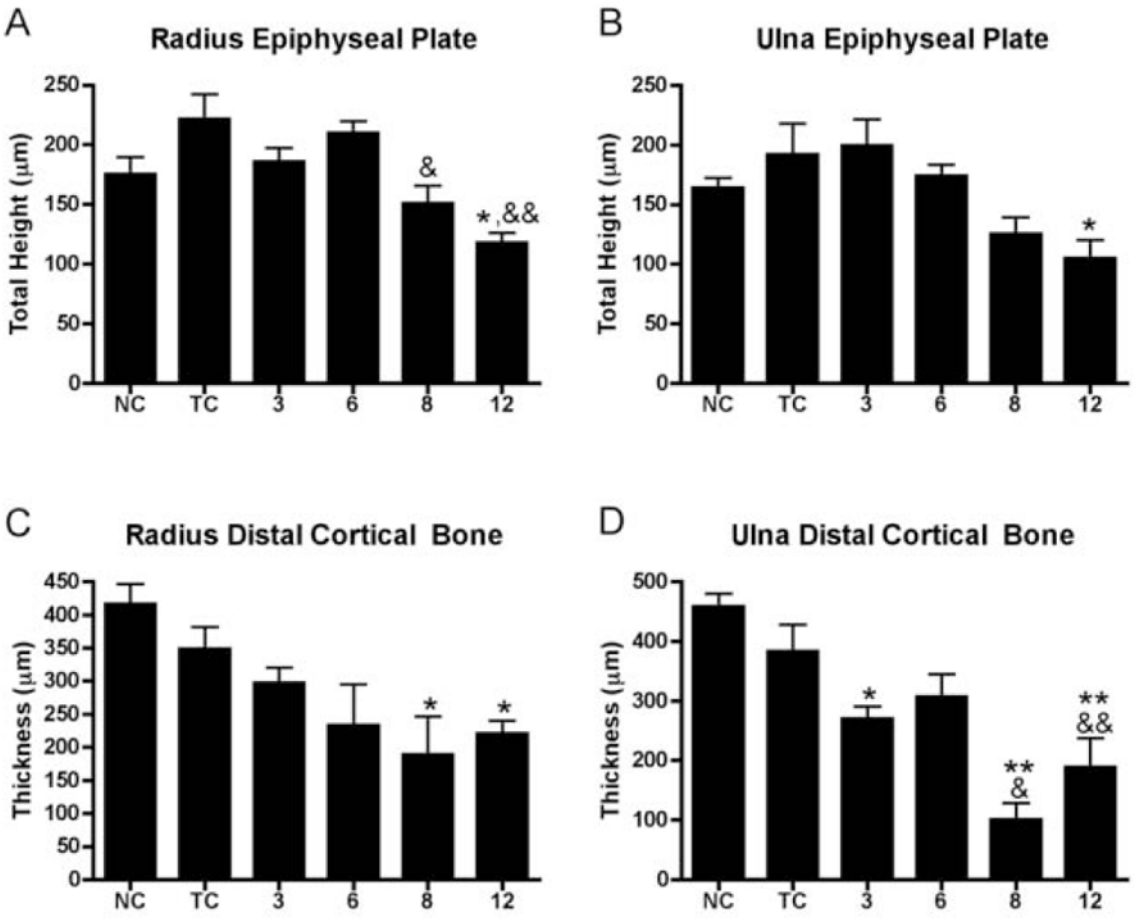

Figure 7.

A–D: Morphological quantification of epiphyseal plate height and cortical wall thickness of the distal radius and ulna of normal control (NC), trained control (TC), and HRHF (3, 6, 8 and 12 wk) animals. (**A**) Epiphyseal plate height was decreased in the distal radius in week 12 compared to normal controls (*: $p<0.05$), and in weeks 8 and 12 compared to trained controls (&: $p<0.05$; &&:$p<0.01$). (**B**) Epiphyseal plate height in the distal ulna was decreased in week 12 compared to normal controls (*: $p<0.05$). **(C)** Distal radius cortical thickness was decreased in weeks 8 and 12 compared to normal controls (*: $p<0.05$; **: $p<0.01$). **(D)** Distal ulna cortical thickness was decreased in weeks 3, 8 and 12 compared to normal controls (*: $p<0.05$; **: $p<0.01$), and compared to trained controls (&: $p<0.05$; &&: $p<0.01$).